An experimental investigation of surface-modified silica nanoparticles in the injection water for enhanced oil recovery

Alberto Bila[1, *], *Jan* Åge Stensen[1, 2], and *Ole* Torsæter[1]

[1]PoreLab Research Center, Department of Geoscience and Petroleum-Norwegian University of Science and Technology (NTNU), S. P. Andersens veg 15a, 7031, Norway
[2]Sintef Industry, S. P. Andersens veg 15a, 7031, Norway

Abstract. Extraction of oil trapped after conventional water flooding still poses huge challenges in the oil industry. Therefore, innovative enhanced oil recovery (EOR) technologies are required to run the production more economically. Recent advances suggest renewed application of surface-modified nanoparticles (NPs) for oil recovery. The advantages of these NPs include improved properties (e.g. stability, stabilisation of emulsions, etc.), which make them appropriate to improve microscopic sweep efficiency of water flood. However, the EOR mechanisms of NPs are not well understood. This work evaluates the effect of four types of polymer-coated silica NPs as additives to the injection water for EOR. The NPs were examined as tertiary recovery agents using water-wet Berea sandstone rocks at 60 °C. Crude oil was obtained from North Sea field. The NPs were diluted to 0.1 wt. % in seawater before injection. The transport behaviour of the NPs and their interactions with the rock system were also investigated to reveal possible EOR mechanisms. The flooding experiments showed that the NPs could effectively increment oil recovery in water-flooded reservoirs. The incremental oil recovery was up to 14% of original oil in place (OOIP). Displacement studies revealed that oil production was affected by interfacial tension reduction and wettability effect; however, the migration behaviour of the NPs through the rock suggested that log-jamming effect and formation of NP-stabilized emulsions were relevant explanations for the mobilisation of residual oil.

1. Introduction

The oil production rates of the existing fields are declining, and the occurrence of new discoveries has been scarce [1, 2]. Therefore, improving the recovery rates from mature oil fields is a priority for oil companies. The oil recovery factor from oil fields is typically around 20-40% of OOIP [3], the remaining oil is in some cases amenable for further developments. However, before the design of any production strategy, it is important to understand the mechanisms that have led to the entrapment of the oil during the early stages of oil production. After secondary water flooding in water-wet reservoirs, oil remains in the larger pores, where it can snap-off and become trapped [4]. This oil or residual oil saturation dwells in the reservoir pore spaces as capillary-trapped and/or by-passed oil [2, 5]. Mobilisation of the capillary-trapped oil requires increasing the viscous forces or decreasing the capillary forces [5, 6]. Increasing the viscous forces may result in fracturing of a reservoir; hence, decreasing the capillary forces becomes an assertive option; this can be achieved through the reduction of interfacial tension between the reservoir fluids. Conversely, the by-passed oil or the oil located in unswept areas of the reservoir can be mobilised by pore plugging and diversion of the normal flow of the injected fluids [5-8].

For this purpose, experimental and numerical studies suggest that properly designed nanoparticles (NPs) can change the physical or chemical behaviour of an oil reservoir, thereby increasing microscopic sweep efficiency of water flood. This is because NPs have small diameter size (1-100 nm) and large surface area-to-volume ratio. These properties enhance the NPs mobility and surface activity, particularly at elevated temperature, thus making them suitable to modifying the fluid-rock properties [9, 10]. Furthermore, NPs can easily travel through and reach untouched zones of a reservoir with no severe impact to the rock permeability [1, 8, 10]. The NPs are injected into the reservoir in the form of suspended particles in designed carrier fluid (e.g. water, ethanol, etc.). The suspension system must remain stable under reservoir conditions throughout the duration of oil recovery process to perform effectively such a task.

Thus far, silica NPs are the most studied nano-materials. They naturally occur in sandstone formations and are costly effective [1, 11]. Additionally, silica NPs can be synthesized and surface functionalised to meet particular reservoir conditions [9, 10].

Promising oil recovery results have been reported in the literature due to silica NPs [11-18] under a variety of experimental conditions. The experiments varied from the

* Corresponding author: alberto.bila@ntnu.no

use of silica NPs with different size, composition, surface functionalities, etc., suspended in aqueous solutions with diverse ionic strength [11-17] or in non-aqueous solutions [16]. The concentration of the NPs in the continuous phase is also varied. Furthermore, the injection flowrate, temperature, evaluation criteria of oil recovery, etc., are often selected randomly, even if the NP suspension system is intended for particular oil field application. The variation of the experiments makes it difficult to adequately grasp the oil recovery mechanisms of silica nanoparticles. Nevertheless, studies aiming at explaining the oil recovery due to silica NPs injection have suggested multiple EOR mechanisms such as; i) interfacial tension (IFT) reduction and wettability alteration [12, 16, 17, 19], ii) structural disjoining pressure [26], iii) formation of in-situ emulsions [20-22], and iv) Pore blocking and microscopic flow diversion [6-8, 14, 23-25].

In nanofluid flooding EOR, NPs are expected to decrease the IFT between the flowing aqueous and oil phases. Thus, promoting deformation and breakup of oil into small drops that can easily be produced. This implies redistribution of flowing fluids within the reservoir and modification of the fluid's relative permeability, which is a manifestation of wettability effect. When there is no tendency for NPs to adhere to the solid surface, the oil recovery occurs through so-called structural disjoining pressure effect proposed by Wasan and Nikolov [26]. Furthermore, the flow dynamics and the interactions occurring between NPs and rock system can boost emulsification of oil. On the other hand, small NPs can block larger pore spaces, prompting the pressure to increase and forcing the injected water to find new paths, resulting in increased oil recovery. Verification of the contribution of each of the proposed NP's mechanisms for oil recovery has not been established yet. More studies are needed to realise optimum conditions for a significant increase in oil recovery to make nanotechnology robust for field applications.

The goal of this work was to evaluate the efficacy of surface modified silica NPs for EOR in water-wet reservoirs and identify possible oil recovery mechanisms. The NPs suspension was prepared at 0.1 wt. % in synthetic seawater. After which, the nanofluids were evaluated as tertiary EOR agents at 60 °C.

2. Experimental materials

2.1 Silica nanoparticles and synthetic seawater

Four types of hydrophilic silica NPs were used. The particles were spherical and hydrophilic with surface coated by polymer molecules to render them stable in synthetic North seawater. The main component of the NPs was silicon dioxide (SiO_2>98.3%), additional components such as aluminium oxide (Al_2O_3) and mixed oxides (MOX) were present. The NPs are special research and development (R&D) products from Evonik Industries and were supplied to us as AERODISP®, which is AEROSIL® particles in liquid solution. The properties of the NPs suspended in distilled water, as received, are given in **Table 1**.

Table 1. Properties of silica NPs dispersed in distilled water.

NF	Basis	wt. %	Size (nm)
02-3	SiO_2 (sol gel cationic)	38.6	107
02-4	SiO_2 (sol gel anionic)	26.0	32
02-6	SiO_2/Al_2O_3/MOX	21.6	218
02-8	SiO_2/Al_2O_3/MOX	25.6	145

The concentrated solutions of the NPs were diluted to 0.1 wt. % in synthetic North seawater (SSW), here referred to as nanofluid (NF). The number in front of "NF" is used to identify the nanofluid type hereafter. The composition of prepared SSW by wt. % was NaCl (74.4), KCl (1.85), $NaHCO_3$ (0.57), Na_2SO_4 (10.62), $CaCl_2 \cdot 6H_2O$ (4.24), $MgCl_2 \cdot 6H_2O$ (8.25) and $Sr_2 \cdot 6H_2O$ (0.07). The total dissolved salts were approximately 38,318 ppm. The density, viscosity and pH of SSW was 1.008 g/cm^3, 0.53 cP and 7.97, respectively. The nanofluid density was 1.007-1.009 g/cm^3 and the viscosity ranged from 0.51-0.67 cP. All measurements were performed at 60 °C using Anton Paar Density meter and Anton Paar Rheometer, respectively

2.2 Oleic phase

A North Sea reservoir crude oil was used in this work. It was a light oil (30 °API, 6 cP at 60 °C) with 71.57 wt. % saturates, 20.81 wt. % aromatics, 7.44 wt. % resins and 0.18 wt. % of asphaltenes. The crude oil was filtered twice through a 5-µm Millipore filter to remove any suspended particles that can block the lines and the pores spaces and or change the oil composition. Normal decane with density of 0.73 g/cm^3 and viscosity of 0.92 cP at 20 °C was used for wettability experiments.

2.3 Core characterization and preparation

Ten core plugs initially at water-wet conditions were used in this work. The cores were drilled from the same block of Berea sandstone; their mineral composition was measured with X-ray diffraction and were composed of 93.7 vol % quartz, 5 vol % of Microcline (Alkali feldspar) and 1.3 vol % Diopside. The core plugs were prepared to have similar dimensions of 3.8 cm diameter and length of 10 cm. They were cleaned with methanol through Soxhlet extractor and then dried at 60 °C for 2-3 days. Afterwards, gas porosity and permeability were measured on dried core plugs. The next step was to evacuate the core plugs for 2 hours and saturate them with SSW at 100 mbar vacuum pressure for 2-3 hours. The saturated cores were left soaked in the same SSW for at least 10 days for ionic equilibration with the rock constituents. The weight of the wet and dried core plugs was used to calculate the porosity and pore volume (PV), and these data are given **Table 2**.

Table 2. Properties of Berea sandstone core plugs.

Core	Porosity (%)	K_{abs}[1] (mD)	PV (ml)
L1	18.7	404	21.4
L2	17.4	537	21.8
L3	15.9	460	17.6
L4	16.2	411	17.9
L5	17.1	367	18.9
L6	16.8	333	18.5
L7	18.4	384	20.3
L8	18.3	184	20.3

[1]Klinkenberg corrected permeability.

2.4 Core flooding equipment

Fig. 1 presents a schematic of core flooding rig with its main components labelled. It utilizes an injection pump, three cylinders containing oil, synthetic sea water and nanofluid each. All cylinders were assembled vertically inside a temperature-controlled oven.

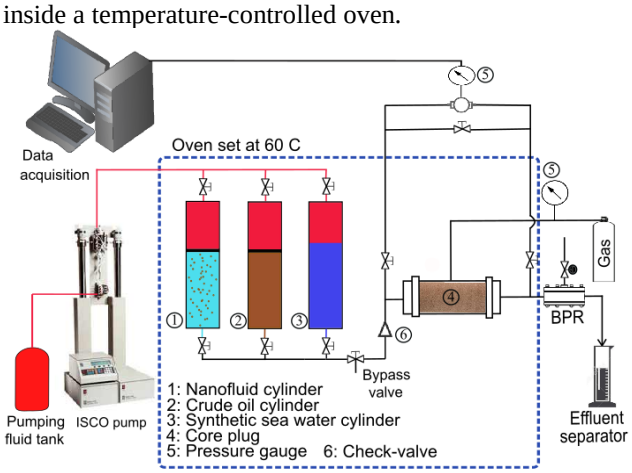

Fig. 1. Schematic of core flooding apparatus.

The core was loaded in the core-holder and oriented horizontally at a confining pressure held within 18-22 bar. A check valve and a backpressure regulator (BPR) were used to prevent back-flow of produced fluids and maintain the pore pressure constant during the core flooding experiments. The BPR was set to 5-bar pressure. The core flooding experiments were performed at 60 °C.

3. Experimental methodology

3.1 Core-flooding

Eight flooding tests were conducted with nanofluids as tertiary EOR-agents (two parallel tests for each nanofluid type). First, the 100% SSW saturated core plug was injected with fresh SSW for 1-2 PVs to ensure a complete removal of gas bubbles. Second, the drainage process was conducted by successively increasing the crude oil injection flowrate, from 0.5, 1.5 to 3 ml/min, for 15 PVs. This procedure ensured that there was no SSW production and the irreducible water saturation (S_{wir}) was achieved. The direction of the injection was reversed after half of the total PVs injected to even the distribution of the fluids within the core. This procedure also established the OOIP reported in **Table 3**. It is worth note that the drainage step was conducted at ambient conditions.

Before starting the experiments, the flooding system was heated while injecting crude oil at low rate of 0.02 ml/min until the temperature stabilised at 60 °C. Then, water (SSW) flood followed at constant flowrate of 0.2 ml/min until there was no oil production for 1-2 PVs. Thereafter, the flowrate was increased ten-fold (bump rate) for ≈1PV to overcome the capillary end-effects. In the following step, the injection was continued with nanofluid at 0.2 ml/min until there was no more oil production for 2-4 PVs. Then, the flowrate was bumped for ≈1PV. During the flooding experiments, the volume of oil produced was collected every ¼ PV and corrected for the flooding system dead volume. When the oil production was occurring at low pace, a camera with automated capturing was used to record the production in a graded line overtime, while the total production was being collected in a large effluent separator. The recorded pictures were then analysed to measure the amount of oil produced overtime. This oil was compared to the total volume of oil produced in the large effluent separator.

The differential pressure (dP) and oil recovery were recorded versus PVs injected, and the residual oil saturation (S_{or}) was calculated for each flooding stage.

3.2 Interfacial tension measurement

The interfacial tension (IFT) between crude oil and SSW or nanofluids was determined with pendant drop and spinning drop techniques at 60 °C.

For the pendant drop method, a Kruss drop shape analyser (DSA) 100 assembled with a J-shape syringe-needle of 1.0047 mm of inner diameter was used to dose the oil drops. With the oil drop hanging from the needle in the bulk phase, the measurements were taken every 20 seconds until static IFT value was reached. The IFT was calculate using Young-Laplace model. For the spinning drop method, a SVT20N (Data Physics) spinning video tensiometer was used. Crude oil was injected drop-wise into a capillary tube filled with SSW or nanofluid. The tube was rotated at speed varying from 6,000 to 10,000 rpm. The IFT was calculated based on the model by Than, et al. [27], at equilibrium. The refractive index measured for both SSW and nanofluids was 1.338.

3.3 Amott-wettability test

The wettability of the cores was evaluated before and after nanofluid flooding at ambient conditions using Amott-test. The core plugs were set at S_{wir} before placing each core plug in the Amott cell filled with SSW. The SSW was allowed to imbibe spontaneously into the core displacing oil over time. The oil production was recorded stepwise until the equilibrium was reached and the total denoted as $V_{o1.}$ The remaining mobile oil (V_{o2}) was forcibly displaced by core flooding method, i.e. by injecting SSW at high flowrates (1 ml/min to 3 ml/min).

Then, the core was removed from the core-holder and dipped in the Amott cell filled with oil to assess whether the oil could spontaneously displace water phase. At equilibrium, the amount of SSW produced was recorded as V_{w1}. The remaining mobile SSW in the core (V_{w2}) was displaced by injecting oil at high flowrates. Decane was used as the oleic phase.

The wettability index (WI) was calculated as the difference between the displacement-by-water ratio (water index, $I_w = V_{o1}/(V_{o1} + V_{o2})$) and displacement-by-oil ratio (oil index, $I_o = V_{w1}/(V_{w1} + V_{w2})$). Categorisation of wettability based on WIs is given in ref. [28]

4. Experimental results

4.1 Oil recovery

Eight core flood tests were conducted at 60 °C. Two core plugs were used for each nanofluid type to reproduce the results and reduce experimental errors. To overcome the capillary end-effects and ensure that any additional oil recovery was a result of nanofluid effect, the flow rate was increased from 0.2 to 2 ml/min at the end of the floods (procedure described in section **3.1**). The oil recoveries achieved by conventional water flooding varied from 47.2 to 56.1% of OOIP. The incremental oil recovery due to nanofluid flooding ranged from 7.0 to 14% of OOIP. The production of first oil due to nanofluid injection was observed for approximately 1.5 to 4 PVs. This was found to depend on NP type, and it was also affected by core properties. Significant oil production was observed after several PVs of nanofluid were injected. An example of oil recovery profile (water and nanofluid flood) at low- and high flow-rates is presented in **Fig. 2** as function of PVs injected for samples NF02-4 and NF02-6. The inset in **Fig. 2a** illustrates the effluent production from nanofluid flooding. It shows the emulsification of oil in water phase, especially when the flowrate was increased during the injection of NF02-4. Alike effluent was observed for sample NF02-3 under the same injection procedure. These samples (NF02-3 and NF02-4) had insignificant effect on pressure compared to the reference case, i.e. the injection pressure remained at the level of water flood pressure (see **Fig. 7a**) throughout the duration of the process.

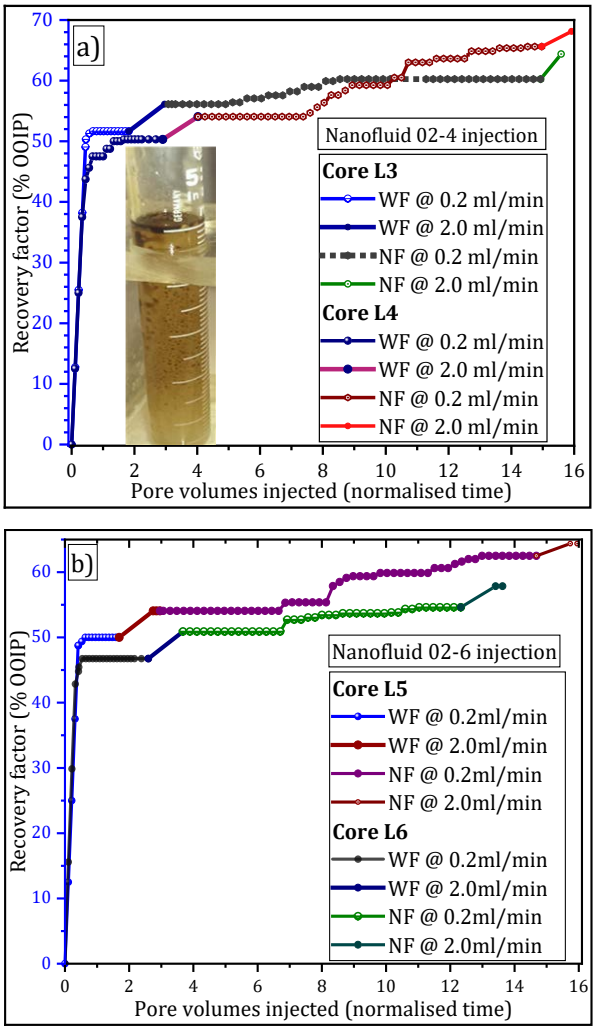

Fig. 2. Oil recovery factors (RFs) versus PVs injected: a) NF02-4 and, b) NF02-6 injection. In both cases, the first oil production was observed after 3 PVs of nanofluids injection.

The injection of NF02-6 and NF02-8 caused the pressure to increase and no visible signs of formation of emulsions were observed, even when the flowrate was increased. The pressure was higher than reference case (see **Fig. 7b).** At the end of the test, a filtered NP "cake" was observed at the core inlet for both NF02-6 and NF02-8 showing that filtration of large NPs and pore blocking was happening during the floods. **Table 3** summarizes

Table 3. Oil recovery factors (expressed as % of OOIP) achieved at each injection rate. The RF_1 and RF_2 represent the oil recovery factors at low flowrate (0.2 ml/min) and high flowrate (2 ml/min), respectively.

NF	Core	S_{wir} (%)	OOIP (ml)	Water flood			S_{or1} (%)	Nanofluid flood			S_{or2} (%)	E_D (%)	Total RF
				RF_1	RF_2	RF		RF_1	RF_2	RF			
02-3	L1	24.7	16.1	44.7	2.5	47.2	39.8	8.6	1.4	9.9	33.6	15.6	57.1
	L2	32.2	14.8	43.9	4.1	48.0	35.3	7.0	4.1	11.1	27.7	22.0	59.1
02-4	L3	10.5	15.7	51.7	4.4	56.1	39.3	5.3	3.0	8.3	31.9	19.0	64.4
	L4	10.6	16.0	50.3	3.8	54.1	41.1	11.6	2.5	14.1	28.5	31.0	68.2
02-6	L5	15.5	16.0	50.0	4.1	54.1	38.8	8.4	1.9	10.3	30.1	22.4	64.4
	L6	16.7	15.4	46.8	4.2	51.0	44.3	4.7	2.3	7.0	35.1	21.0	58.0
02-8	L7	18.8	16.5	49.4	4.2	53.6	37.7	8.2	0.9	9.1	30.0	20.4	62.7
	L8	18.7	16.5	52.4	2.7	55.2	36.5	7.3	3.0	10.3	28.1	23.0	65.5

the main core flooding results used to evaluate the nanofluid samples. The displacement efficiency due to nanofluid was evaluated by equation:

$$E_D = \left[1 - \left(\frac{S_{or2}}{S_{or1}}\right)\right] \times 100\% \quad (1)$$

Here, S_{or1} and S_{or2} represent the residual oil saturation at the end of water- and nanofluid-flooding (low and high flow rate injection), respectively.

4.2 Interfacial tension

The interfacial tension (IFT) between crude oil and NF02-3 and NF02-4 was measured with both pendant drop and spinning drop methods. Nanofluids NF02-6 and NF02-8 were very sensitive at elevated temperature; the solutions immediately precipitated at 60 °C and became opaque, thus making it impossible to use the pendant drop method for IFT analysis. The spinning drop was used instead. **Fig. 3** shows the crude oil drop hanging from a needle within sample NF02-6 at 22 °C and 60 °C. When the temperature was increased, the NPs quickly agglomerated at the oil and water (o/w) interface. The agglomerates or layers of NPs deposited on the bottom of the cuvette due to gravity force.

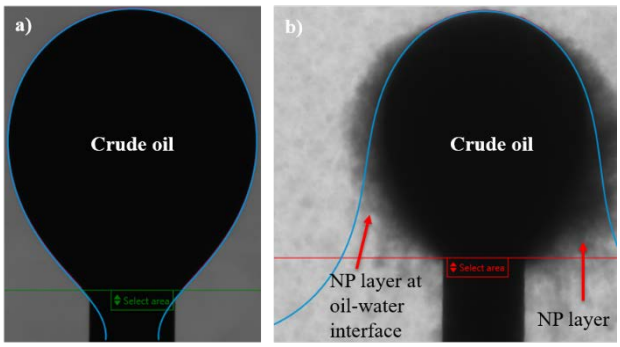

Fig. 3. Crude oil drop suspended in NF02-6: a) at 22 °C, and b) at 60 °C, NPs self-assembled at the w/o interface.

This effect was viewed thanks to a high-resolution pendant drop camera. The measured values of interfacial tension are presented in **Table 4**.

Table 4. Interfacial tension values measured at 60 °C.

Fluid	Interfacial tension (mN/m)	
	Pendant drop	Spinning drop
SSW	11.0	10.0
NF02-3	3.5	3.1
NF02-4	3.3	2.9
NF02-6	-	6.8
NF02-8	-	4.7

The spinning drop was also used to confirm the IFT values obtained from pendant drop method for samples NF02-3 and NF02-4. **Fig. 4** shows a crude oil droplet dipped in the capillary tube spun at 7,000 rpm and at 60 °C. Due to the high rotational speed, there were no visible aggregates of NPs and the IFT could be measured for all samples.

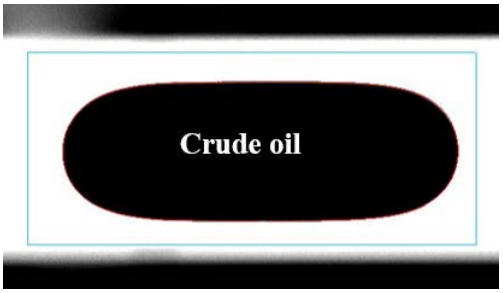

Fig. 4. Crude oil drop shape inside the capillary tube filled with NF02-6 and spun at 7,000 rpm for IFT analysis using STV20 spinning drop video tensiometer.

4.3 Core wettability

Two core plugs were used to investigate the initial wettability of the cores (i.e. before nanofluid injection). The measured wettability index of the cores was, WI = 0.86, on average, showing strongly water-wet condition. The core plugs used afterwards were considered water-wet. This assumption was made because all the core plugs were drilled from the same block and followed the same preparation and cleaning procedures.

After nanofluid flooding was completed, each core (at S_{or}) was flooded with decane using high flowrates (1 to 3 ml/min) until residual nanofluid saturation was achieved. Thereafter, each core plug was dipped into the Amott cells following the procedure described in section **3.3**. **Fig. 5** shows the oil recovery from SSW spontaneous imbibition (SI) during 30-days test. It was observed that the rate of water imbibition decreased slightly in cores injected with nanofluids compare with original ones (not injected with NPs). At the beginning of the test, the oil was produced from all the faces of the core plugs.

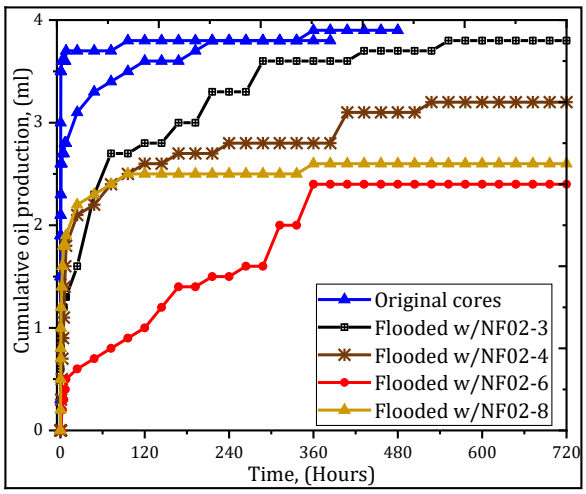

Fig. 5. Water spontaneous imbibition performed on cores flooded with nanofluids (at ambient conditions).

After 2-3 days, the oil production was observed from the top of the core plugs. The produced oil, at this stage,

* Corresponding author: alberto.bila@ntnu.no

remained on the top surface of the cores and detached from it after several days or by gently shaking the Amott cells. These events are depicted by rapid increase in oil recovery at some points in **Fig. 5**. At equilibrium, the measured water indexes (I_w) varied from 0.5 to 0.89.

In the second cycle of spontaneous imbibition, oil did not imbibe into the core or displace water, implying that the Amott oil index is zero, $I_o = 0$. Therefore, the Amott-test was not completed, and the obtained water indexes were used to assess the effect of NPs on the rock surface.

4.4 Permeability and porosity

After nanofluid flooding and wettability evaluation tests, the cores were cleaned with toluene and methanol for several days with Soxhlet extraction and dried at 60 °C for 2-3 days. Then, the gas permeability and porosity were measured. The results are presented in **Table 5**. The objective was to determine and quantify the changes of initial values of permeability and porosity as result of NPs adsorption or retention during the nanofluid flooding process. The negative values, in **Table 5**, indicate permeability or porosity impairments; otherwise, it would indicate improvement.

5. Discussion of the results

5.1 Nanofluid stability analysis

The approaches used to study the stability of the NPs solutions at 0.1 wt. % were: i) the particle size distribution (PSD), ii) zeta potential, and iii) sedimentation test.

Malvern Zetasizer instrument was used to characterise the PSD and zeta potential of the NP solutions. After setting the temperature at 60 °C, the average particle diameter size for NF02-3 was 94 nm and 32 nm for NF02-4. A comparison of the measured particle size shows that the size is in the range claimed by manufacturer (i.e. 107 nm for NF02-3 and 32 nm for NF02-4). Hence, it suggests that the NPs were stable in seawater solution, at least for the measured period. The measurements for samples NF02-6 and NF02-8 resulted in high values of polydispersity index indicating formation of large NP aggregates, thus not suitable for the characterisation of particle size with dynamic light scattering technique. The measurements of zeta potential of the NPs gave unreliable values, for unknown reasons.

Visual observations were conducted to confirm the results obtained from particle size measurements. The nanofluids were placed in the oven at 60 °C and monitored daily. It was immediately observed that NF02-6 and NF02-8 were aggregating at 60 °C, as also noted during measurements of interfacial tension. The formed NPs structures deposited to the bottom of the ampules within the couple of hours. The stability analysis for NF02-3 and NF02-4 was conclusive after 4 days. After which, the nanofluid samples also started to flocculate and gradually settled out of solution and forming large NPs aggregates. **Fig. 6** illustrates the NPs in the aggregated form on the bottom of the ampules (white) after four-day test. It was interesting to observe, visually, (for sample NF02-4) the stretching and flocculation of polymer chains in solution. Possibly, this was caused by hydrolysis and the polymers precipitated in the presence of divalent cations (e.g. Mg^{2+}, Ca^{2+}) at the elevated temperature [29]. Consequently, the desired repulsion forces between the NPs in the solution vanished between the particles.

Fig. 6 Visual analysis of NPs stability. The white colour at the bottom of each ampule indicates the aggregated NPs. Stretched polymers in SSW were observed in NF02-4.

Table 5. Permeability and porosity measured before and after nanofluid flooding on core plugs.

Core	Injected nanofluid	Permeability (mD)			Porosity[2] (%)		
		before	after	% difference	before	after	% difference
L1	02-3	404	350	-13	19	17	-10
L2		537	452	-16	20	16	-19
L3	02-4	460	446	-3	17	15	-11
L4		411	370	-10	18	16	-15
L5	02-6	367	232	-37	18	13	-25
L6		331	246	-26	18	14	-25
L7	02-8	384	292	-24	18	15	-18
L8		265	193	-20	20	17	-16

[2]Measured with Helium porosimeter

Based on sedimentation test, it was concluded that NF02-3 and NF02-4 were stable for approximately 4 days whereas NF02-6 and NF02-8 became readily unstable at 60 °C. The primary observation is that the injection of these NPs will increase the pressure and oil production costs. Therefore, they may not be suitable for EOR at field-scale. Therefore, the surface modification of these particles still needs to be optimized to remain stable for extended periods of injection (expected at field-scales). This should not only focus on the particle stability, but also on the surface chemistry and other possible interactions that may occur between NPs and an oil-field.

5.2 Evaluation of oil recovery

An accurate evaluation of tertiary oil recovery not only requires the reproducibility of experimental results, but also to properly determine the waterflood S_{or} and to ensure that any additional oil is solely due to EOR effect. To achieve this, twin core plugs were used for each nanofluid type; the injection of water at low rate was changed after it did not produce more oil for 1-2 PVs, thereafter the flowrate was bumped for 1 PVs.

It was observed that the nanofluids at a concentration of 0.1 wt. % could mobilise the residual oil, but it was delayed compared to breakthrough of nanofluids. The arrival of first oil at the core outlet varied among the samples. It occurred after 1.5 to 4 PVs were injected of nanofluids. The oil production due to NF02-6 (**Fig. 2b**) and NF02-8 was observed at late injection times compared to NF02-3 and NF02-4 (**Fig. 2a**); at this stage, the produced oil consisted of small droplets that merged with the oil in the separator. For all samples, the main oil occurred after large amount of nanofluid were injected. In **Fig. 2**, we see several points were oil increases due to nanofluid injection. The amount of oil recovered stepwise varied as the NPs injection advanced and the NPs interacted with the rock system. The late occurrence of oil production with nanofluid injection is attributed to differences between the viscosities of nanofluids and crude oil ($\mu_o/\mu_{nanofluid} \approx 6$). Additionally, oil production was affected by number of pore volumes injected during the water flood stage and variations in core properties. Therefore, for the nanofluids to produce an additional oil, an extra energy or physicochemical interactions between the nanoparticles and the oil system was needed. This shows that injected NPs in the reservoir need to decrease the surface energy to deform and break large oil drops and/or to block enough pores to build up enough pressure across the core to detach and mobilise the residual oil in the adjacent pores.

Despite the late occurrence of oil production, the core flooding tests have revealed that surface modified silica NPs can extract more oil efficiently in water-wet water flooded Berea sandstone formations. The EOR potential of the NPs was revealed after the injection of large amounts of nanofluids. However, if these results are directly compared to a field-scale injection, it may appear economically unfeasible because of the cost of NPs. But, to better simulate the injections at field-scale, large pore volumes of nanofluids must be injected at core scale [30].

Table 3 reports the oil recoveries achieved at the end of water and nanofluid flooding. The oil recovery achieved by water flood varied from 47.2% to 56.1% of OOIP after the flowrate was bumped. When the nanofluid system was injected at low rate, the incremental oil recovery varied from 4.7% to 11.6% of OOIP. Increasing the flowrate tenfold for ≈1 PV, the ultimate incremental recoveries reached 7.0% to 14.1% of OOIP. The oil recovery during the bump rate is shown in **Fig. 2** by a "linear" segment. This was because it was difficult to record the amount of oil produced per step during the bump rate, as it was a quick and short process. Additionally, oil was produced as droplets. Therefore, the total volume of oil was measured at the end of injection and added to that recovered at low rate injection. It should be noted that the "linear" segments in **Fig. 2** do not indicate linear production of oil.

The twin cores produced comparable results; the variation was below 5%. The thin gap between the core plug and the end plug may be the main source of capillary end effects, thus affecting the obtained results. In addition to the core heterogeneity and the criteria chose to switch from low to high rate (2 PVs of no oil production), probably it was not optimal to reach the equilibrium. Consequently, additional oil production may occur with the bump rate (producing bypassed oil in the core).

Conjugating the data from **Table 1** and **Table 3**, one can see that the highest incremental oil recovery was achieved by the smallest NPs size. The increased oil recovery with decreasing the NP size is also consistent with measured IFT values shown in **Table 4**, where it is shown that NPs of small size were efficient in lowering the o/w interfacial tension, thus resulting in higher oil recovery than the large sized NPs. The results are also in agreement with previous findings reported in the literature [13, 20], but are also in contrast to the positive correlation observed between the NP size and oil recovery reported by Aurand, et al. [23]. The NPs at 0.1 wt.% had no significant effect on the viscosity of the SSW solution, thus unable to improve the mobility ratio. The maximum pressure was achieved from NPs of large size. This observation supports the notion that increasing the NPs size decreases the rock permeability [13], and reduces the surface functionalities of the NPs at the oil-water-rock interfaces [31, 32], thus resulting in low oil recovery.

The small variations observed in oil recoveries (<5%) ensured reproduced results in this work; it proved that the surface-modified silica NPs can improve oil recovery efficiently in water-wet water flooded reservoirs under the experimental conditions.

5.3 Evaluation of EOR mechanisms

This work reports promising results for the application of surface-modified silica NPs for EOR. In section **1**, we reviewed possible mechanisms of silica NPs based on the mechanisms responsible for entrapping the oil after water flooding in water-wet reservoirs. We observed that for each nanofluid type different recovery mechanisms are

operating for maximum oil recovery. This implies that additional studies are needed to quantify the contribution of the involved EOR mechanisms. The actual oil recovery mechanisms are discussed in the following sections to gain knowledge and suggest the probable dominant mechanisms of the surface modified nanoparticles

5.3.1 Interfacial tension and rock wettability

In nanofluid flooding applications, NPs are needed to improve water flooding microscopic sweep efficiency. When injecting the NPs, the major expectation is that the differential pressure across the core exceed the capillary forces trapping the oil. This can be achieved if the NPs adsorb to the o/w interface, which will in turn decrease the IFT between oil and injection water. Capillary number, N_c, describes the balance between the oil mobilising forces (viscous forces) and the oil trapping forces, and it provides a mean to evaluate how effective the NPs are for mobilizing the residual.

$$N_c = \frac{\mu\nu}{\gamma} \quad (2)$$

Here, μ and ν are the viscosity and velocity of the displacing fluid, respectively, and ɣ is the interfacial tension between the displacing and displaced phases.
The N_c for water flooding calculated in this work is of order of 10^{-6}. It is generally recognized that the critical capillary number for the onset of mobilization of residual oil in water-wet reservoirs is of orders of $\approx 10^{-5}$ [8, 33] above which, a complete mobilisation of residual may take place. Moreover, this condition can be met if any additive to the injection fluid can decrease the IFT between oil and water down to $<10^{-3}$ mN/m [34].

In this work, it was observed that the modified silica NPs reduced the o/w interfacial tension. In **Table 4**, one can see that the nanofluids had a moderate effect on the o/w interfacial tension, and the IFT values are not low enough to produce the desired N_c to significantly mobilise the residual oil. These findings are consistent with earlier research [23, 35]. The current results indicate poor surface activity performance of the NPs onto the o/w interface. The reasons for that might be i) the high temperature that increased the degree of collision between the NPs in solution and the aggregation tendency at the o/w interface (see **Fig. 3**); ii) the surface modification with polymer was lost due to solubility effect of polymers in water, especially at elevated temperature, thus destabilizing the silica particles in the presence divalent ions. Particularly, the aluminium present in samples NF02-6 and NF02-8 would form sulphates in the solution and prompting the formation of precipitates.

In addition to decreasing the oil and water IFT, the injection of nanofluids explored the interactions occurring at the fluid-rock interface. This is because NPs can modify the fluid distribution and flow-ability of fluids within the reservoir and improve the microscopic displacement efficiency. For this purpose, we explored the rate of water imbibition and the Amott indexes to evaluate the effect of the injected NPs on the solid surface. From **Fig. 5**, one can see that the rate of water imbibition was relatively low especially on cores flooded with samples NF02-3 and NF02-6 compare with original cores (not injected with NPs). Furthermore, we see a sudden increase in oil recovery with time from all the cores indicating a progressive alteration of wettability. This indicates that the adsorbed oil was released as the pore spaces became increasingly water-wet due to NPs, thus resulting in increased oil recovery by spontaneous water imbibition. The measured Amott water indexes ranged from 0.5 to 0.86. The overall results suggest that the wettability was affected by nanofluids to water-wet condition. These results were expected because the injected NPs were hydrophilic, and when exposed to a substrate of like wettability or surface charge such as Berea sandstone, they could adsorb physically or confine themselves on the pores in response to the applied injection pressure. Thus, developing new hydrophilic surface roughness on the pores where the particles were lodged. This results show agreement with previous studies [14, 36] that studied the wettability alteration using hydrophilic silica NP types.

Owing to small effects of NPs on IFT and wettability alteration, the studied NPs are not expected to mobilise residual oil and increase oil recovery by solely reducing the IFT and/or by affecting the wettability. But, the moderate effect of NPs on fluid-rock properties still plays a predominant role for stabilisation of emulsions [21, 37, 38]. This effect or the emulsion formation will be discussed in the following section, especially for samples NF02-3 and NF02-4, that achieved the lowest IFT reduction among the studied nanoparticles.

5.3.2 Differential pressure profile analysis

The differential pressure (dP) was recorded during the flooding experiments using a Keller PD-33X with range of 0-30 bar instrument. The dP behaviour may indicate whether emulsions were formed [20] or microscopic flow diversion was occurring during NPs flooding. Gathering these data one can comprehend the migration behaviour and the EOR mechanisms of NPs.

During the flood of nanofluids NF02-3 and NF02-4, it was observed that the dP increased slightly for ≈1PV, then it decreased and finally it levelled to the reference waterflood value. This behaviour of dP is presented in **Fig. 7a** for NF02-4. The slow rise of dP is thought to be caused by physical confinement of the particles at the core entrance. Then, the pressure decreased as the injection advanced indicating propagation of the NPs through the pore spaces without clogging or causing significant damage to the rock permeability. The reduction of core absolute permeability varied from 3% to 16%, which confirmed low retention and the ease with which the NPs travelled through the core. Furthermore, the low pressure also provided an indication of generation of in-situ emulsions with nanofluid flooding. This was confirmed by increasing the flowrate; oil-in-water emulsions were visible in the effluent vials as illustrated by the inset picture in **Fig. 2a.** The yellowish colour of the effluent is attributed to the solubilisation of oil during the

displacement process. The collected effluent production contained significant fraction of discrete oil droplets in the water phase. These droplets merged upwards with the oil in the vials after a couple of hours due to gravity effect. Previous studies that investigated the EOR effect of polymer-coated silica NPs, such as used in this work, have highlighted the formation of NPs-stabilised emulsions for oil recovery. The studies argued that NP-stabilized emulsions can easily be transported out of the cores with low retention, and increase oil recovery [14, 21, 37].

The generation of emulsions, in this work, concurs with the reduction of IFT, especially for NF02-3 and NF02-4 (with the lowest IFT reduction among the studied samples). In addition to the high temperature that was enhancing the oil and water interactions within the core resulting in flow of emulsion, particularly, when the flowrate was increased. This is because increasing the flowrate can provide an extra energy required to break up oil phase, thus allowing more NPs to adsorb at the oil-water interface [22]. Additionally, NF02-3 and NF02-4 had surfactant agents present in their composition, thus favourable to generating emulsions. It is most likely that samples NF02-3 and NF02-4 improved oil recovery by affecting the effective mobility to oil (oil relative permeability) due to generation of NP-stabilised oil-in-water emulsions.

The contrasting results were observed during the injection of samples NF02-6 and NF02-8, little to no formation of emulsions were observed, even with the increased flowrate. The injection of these samples was accompanied with continuous increased pressure. From approximately 5 PVs of nanofluid injection the dP showed high degree of oscillation until the tests were stopped. At the end of the flooding test, a filtered NP "cake" was observed at the core inlet indicating that a cross-flow filtration, blockage of the pores was occurring, which is likely the primary source for pressure increase. This is because the NPs were hydrated and were unstable in SSW, so the particle size has increased and creating favourable conditions for blockage of small pores from start of the injection. An example of the pressure profile is shown in **Fig. 7b**; the inset picture illustrates the formed filtered NP "cake" due to NF02-6. Accordingly, the permeability reduction was in the range of 20% to 37%, and it was higher than that measured on cores injected with samples NF02-3 and NF02-4. As mentioned earlier, NF02-6 and NF02-8 produced the first oil at the latest injection time of all tested NFs and progressively increased pressure. The pressure pattern also indicated that pore blocking was also happening inside the core until an extreme pore blockage was reached. The effect of pore blocking is likely the diversion of the injection water and the mobilization of bypassed residual oil. **Fig. 7b** also shows periods of an abrupt increase and decrease of dP caused by pore blockage and un-blockage of the jammed NPs. These periods of high spikes (pump effect) supported the notion that the NPs were further retained or aggregating within the core; as a result, the pressure was redistributed within the pores to assist the diverted water to reach and detach the by-passed oil in the adjacent pores.

As the production of oil and the detachment of weakly adsorbed NPs on the pore walls was occurring, the local pore pressure was temporarily relieved. Thus, restoring the normal flow of water. This behaviour was reflected on events of sudden pressure drops (in **Fig. 7b)**. As the blockage continued on the available pore channels, the injected water was continuously forced to find new paths. Due to the high pressure generated with advancing of the injection and subsequent confinement of NPs in the pores, the oil was detached from the surface and produced before the pores were relocked. However, not all cases the pressure increase was accompanied by oil production.

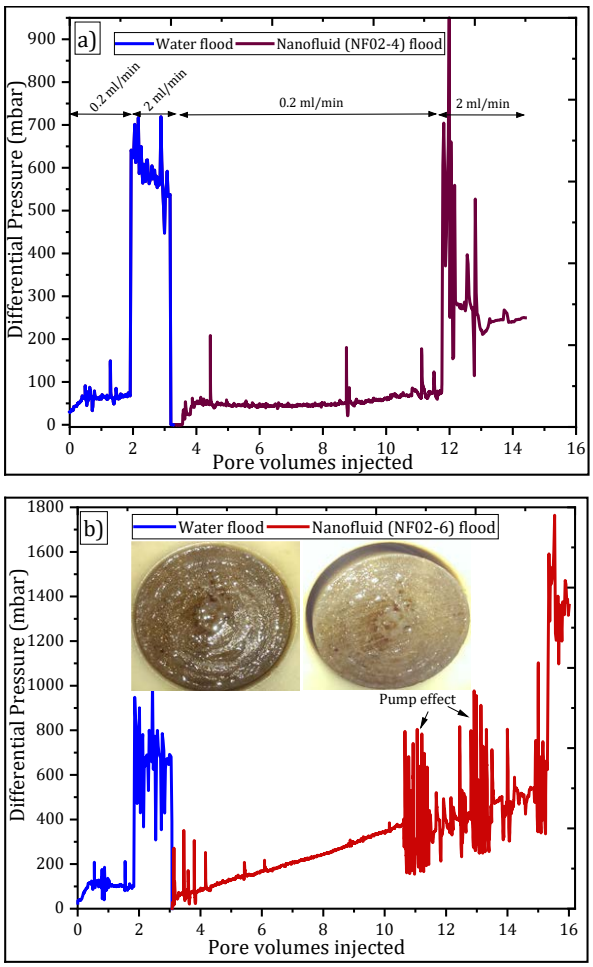

Fig. 7. Differential pressure profiles as a function of PVs of injected fluids: a) NF02-4 injection and b) The inset is the NPs "cake" formed at the core inlet during the injection of NF02-6.

The primary recovery mechanisms for NF02-6 and NF02-8 is possibly the pore blocking and flow diversion also referred to as log-jamming effect [7, 8, 23]. According to Spildo, et al. [5] and Skauge, et al. [7] this phenomenon can be explained by mass difference between the NPs and water. This is because the hydrated NPs become heavy and their flow ability is decreased, hence causing the particles to accumulate at the pore entrance during the core injection. In this work, the log jamming effect finds further support because the NPs were aggregating in SSW solution before the injection. Therefore, further injection would promote accumulation and retention of NPs at the core inlet and within the core

and increase the pressure. The main particle retention mechanism is mechanical rather than chemical adsorption. This is supported by the late occurrence oil recovery and subsequent increased oil production with progressive increase in pressure during the flood process.

Due to the synergistic effect of IFT reduction and wetting effect, the increased dP also contributed for the mobilization of both by-passed and capillary-trapped oil. However, quantifying the contribution of pore blocking and fluid flow diversion mechanisms in the mobilisation of residual oil based on differential pressure is complex.

5.4 Effect of NPs on permeability and porosity

To evaluate the influence of NPs on rock properties, the permeability and porosity were evaluated after nanofluid flooding. The results are presented in **Table 5**. The results revealed both permeability and porosity reduction for all cores after nanofluid flooding. This was due to retention or adsorption of NPs within the cores. The cores injected with nanofluids containing small-sized NPs diameter (NF02-3 and NF02-4) resulted in the lowest reduction in permeability and porosity. The observed permeability reduction was from 3% to 16% and the porosity reduction ranged from 10% to 19%. For these samples the retention may be due to chemical adsorption of NPs owing to their small size [12]. The slightly high values of porosity reduction suggested that adsorption and blockage due to NPs were relevant in the large pores.

Nanofluids NF02-6 and NF02-8 with large initial size and tendency to form large structures of NPs resulted in the largest permeability and porosity impairments. The permeability reduction was from 20% to 37% and the porosity reduction was from 16% to 25%. As the NPs aggregated before the injection, significant permeability and porosity reductions were expected. It is possible that the NPs were desorbed from the pore walls and produced during the preparation of the cores for wettability tests.

6. Conclusions

This work investigated the effect of surface-modified silica NPs for enhanced oil recovery applications. Flooding experiments were performed by injecting the nanofluids in water-wet core plugs at 60 °C in tertiary recovery mode. The NPs were prepared at 0.1 wt. % in seawater. The main EOR mechanisms due to silica NPs were also evaluated. Based on the experimental results, the following conclusions were obtained:

- The core flooding experiments have shown that oil recovery is enhanced with surface modified silica nanoparticles, despite the limited stability. The NPs increased oil recovery up to 14% of OOIP in water-wet rocks at 60 °C;
- The IFT between water and crude oil was decreased with surface modified silica NPs, but the reduction is not in orders of magnitude to contribute significantly to the remobilisation of residual oil;
- The wetting properties of Berea sandstone rocks were moderately affected with nanoparticles towards to water-wet condition;
- An analysis of EOR mechanisms of the studied nanofluid systems suggest that NF02-3 and NF02-4 improved microscopic sweep efficiency by generation of in-situ oil-in-water emulsions, while NF02-6 and NF02-8 recovered oil by pore blocking and microscopic flow diversion (log-jamming effect).

Based on the current findings, further work is underway aiming at evaluating the EOR potential of the same NPs in neutral-wet cores and improving the evaluation procedure of oil recovery mechanisms of the nanoparticles.

Acknowledgements: The authors gratefully acknowledge Evonik Industries for providing the nanoparticles used in this work and the Research Council of Norway for their financial support through PoreLab, Centre of Excellence, project number 262644.

References

1. X. Sun, Y. Zhang, G. Chen, and Z. Gai, "Application of Nanoparticles in Enhanced Oil Recovery: A Critical Review of Recent Progress," *Energies*, vol. 10(3), 2017, pp. 345.
2. A. Muggeridge *et al.*, "Recovery rates, enhanced oil recovery and technological limits," *Philosophical transactions. Series A, Mathematical, physical, and engineering sciences*, vol. 372(2006), 2014, pp. 20120320-20120320.
3. I. Sandrea and R. Sandrea, "Recovery factors leave vast target for EOR technologies," *Oil & Gas Journal*, vol. 105(41), 2007, pp. 44-47.
4. W. Abdallah *et al.*, "Fundamentals of wettability," *Technology*, vol. 38(1125-1144), 1986, pp. 268.
5. K. Spildo, A. Skauge, M. G. Aarra, and M. T. Tweheyo, "A New Polymer Application for North Sea Reservoirs," *SPE Reservoir Evaluation & Engineering*, vol. 12(03), 2009, pp. 427-432.
6. M. A. E. Kokubun, F. A. Radu, E. Keilegavlen, K. Kumar, and K. Spildo, "Transport of Polymer Particles in Oil–Water Flow in Porous Media: Enhancing Oil Recovery," *Transport in Porous Media*, vol. 126(2), 2018, pp. 501-519.
7. T. Skauge, K. Spildo, and A. Skauge, "Nano-sized Particles For EOR," in *SPE Improved Oil Recovery Symposium*, Tulsa, Oklahoma, USA, 2010, pp. 10. https://doi.org/10.2118/129933-MS.
8. Z. Hu, S. M. Azmi, G. Raza, P. W. J. Glover, and D. Wen, "Nanoparticle-assisted water-flooding in Berea sandstones," *Energy & Fuels*, vol. 30(4), 2016, pp. 2791-2804.
9. S. Ayatollahi and M. M. Zerafat, "Nanotechnology-Assisted EOR Techniques:

New Solutions to Old Challenges," in *SPE International Oilfield Nanotechnology Conference and Exhibition*, Noordwijk, The Netherlands, 2012, pp. 15. https://doi.org/10.2118/157094-MS.
10. M. V. Bennetzen and K. Mogensen, "Novel Applications of Nanoparticles for Future Enhanced Oil Recovery," in *International Petroleum Technology Conference*, Kuala Lumpur, Malaysia, 2014, pp. 14. https://doi.org/10.2523/IPTC-17857-MS.
11. M. I. Youssif, R. M. El-Maghraby, S. M. Saleh, and A. Elgibaly, "Silica nanofluid flooding for enhanced oil recovery in sandstone rocks," *Egyptian Journal of Petroleum*, vol. 27(1), 2018, pp. 105-110.
12. M. Zallaghi, R. Kharrat, and A. Hashemi, "Improving the microscopic sweep efficiency of water flooding using silica nanoparticles," *Journal of Petroleum Exploration and Production Technology*, vol. 8(1), 2018, pp. 259-269.
13. L. Hendraningrat, S. Li, and O. Torsater, "Effect of Some Parameters Influencing Enhanced Oil Recovery Process using Silica Nanoparticles: An Experimental Investigation," in *SPE Reservoir Characterization and Simulation Conference and Exhibition*, Abu Dhabi, UAE, 2013, pp. 10. https://doi.org/10.2118/165955-MS.
14. B. A. Suleimanov, F. S. Ismailov, and E. F. Veliyev, "Nanofluid for enhanced oil recovery," *Journal of Petroleum Science and Engineering*, vol. 78(2), 2011, pp. 431-437.
15. K. Xu, D. Agrawal, and Q. Darugar, "Hydrophilic Nanoparticle-Based Enhanced Oil Recovery: Microfluidic Investigations on Mechanisms," *Energy & Fuels*, vol. 32(11), 2018, pp. 11243-11252.
16. N. A. Ogolo, O. A. Olafuyi, and M. O. Onyekonwu, "Enhanced Oil Recovery Using Nanoparticles," in *SPE Saudi Arabia Section Technical Symposium and Exhibition*, Al-Khobar, Saudi Arabia, 2012, pp. 9. https://doi.org/10.2118/160847-MS.
17. L. Hendraningrat, S. Li, and O. Torsæter, "A coreflood investigation of nanofluid enhanced oil recovery," *Journal of Petroleum Science and Engineering*, vol. 111(2013, pp. 128-138.
18. A. Bila, Å. J. Stensen, and O. Torsæter, "Experimental Investigation of Polymer-Coated Silica Nanoparticles for Enhanced Oil Recovery," *Nanomaterials*, vol. 9(6), 2019.
19. R. Li, P. Jiang, C. Gao, F. Huang, R. Xu, and X. Chen, "Experimental Investigation of Silica-Based Nanofluid Enhanced Oil Recovery: The Effect of Wettability Alteration," *Energy & Fuels*, vol. 31(1), 2017, pp. 188-197.
20. M. Adil, K. Lee, H. M. Zaid, N. R. A. Latiff, and M. S. Alnarabiji, "Experimental study on electromagnetic-assisted ZnO nanofluid flooding for enhanced oil recovery (EOR)," *PloS one*, vol. 13(2), 2018, pp. e0193518.
21. T. Zhang, D. Davidson, S. L. Bryant, and C. Huh, "Nanoparticle-Stabilized Emulsions for Applications in Enhanced Oil Recovery," in *SPE Improved Oil Recovery Symposium*, Tulsa, Oklahoma, USA, 2010, pp. 18. https://doi.org/10.2118/129885-MS.
22. I. Kim, A. J. Worthen, K. P. Johnston, D. A. DiCarlo, and C. Huh, "Size-dependent properties of silica nanoparticles for Pickering stabilization of emulsions and foams," *Journal of Nanoparticle Research*, vol. 18(4), 2016, pp. 82.
23. K. R. Aurand, G. S. Dahle, and O. Torsæter, "Comparison of oil recovery for six nanofluids in Berea sandstone cores," in International Symposium of the SCA, France, 2014, vol., no., pp. 1-12.
24. A. I. El-Diasty and A. M. Aly, "Understanding the Mechanism of Nanoparticles Applications in Enhanced Oil Recovery," in *SPE North Africa Technical Conference and Exhibition*, Cairo, Egypt, 2015, pp. 19. https://doi.org/10.2118/175806-MS.
25. A. Bila, J. Å. Stensen, and O. Torsæter, "Experimental Evaluation of Oil Recovery Mechanisms Using a Variety of Surface-Modified Silica Nanoparticles in the Injection Water," in *SPE Norway One Day Seminar*, Bergen, Norway, 2019, pp. 19. https://doi.org/10.2118/195638-MS.
26. D. T. Wasan and A. D. Nikolov, "Spreading of nanofluids on solids," *Nature*, vol. 423(6936), 2003, pp. 156-159.
27. P. Than, L. Preziosi, D. D. Josephl, and M. Arney, "Measurement of interfacial tension between immiscible liquids with the spinning road tensiometer," *Journal of colloid and interface science*, vol. 124(2), 1988, pp. 552-559.
28. W. G. Anderson, "Wettability Literature Survey Part 5: The Effects of Wettability on Relative Permeability," *Journal of Petroleum Technology*, vol. 39(11), 1987, pp. 1453-1468.
29. R. S. Seright, A. Campbell, P. Mozley, and P. Han, "Stability of Partially Hydrolyzed Polyacrylamides at Elevated Temperatures in the Absence of Divalent Cations," *SPE Journal*, vol. 15(02), 2010, pp. 341-348.
30. K. H. Hosseinzade and O. Torsæter, *Injected pore volume on lab and field scales* (9th International Conference on Porous Media & Annual Meeting). Rotterdam, Netherlands: International Society for Porous Media, Interpore, 2017.
31. A. Habibi, M. Ahmadi, P. Pourafshary, s. Ayatollahi, and Y. Al-Wahaibi, "Reduction of Fines Migration by Nanofluids Injection: An Experimental Study," *SPE Journal*, vol. 18(02), 2012, pp. 309-318.
32. P. Bacchin, Q. Derekx, D. Veyret, K. Glucina, and P. Moulin, "Clogging of microporous channels networks: role of connectivity and

tortuosity," *Microfluidics and Nanofluidics*, vol. 17(1), 2014, pp. 85-96.
33. K. J. Humph ry, B. M. J. M. Suijkerbuijk, H. A. van der Linde, S. G. J. Pieterse, and S. K. Masalmeh, "Impact of Wettability on Residual Oil Saturation and Capillary Desaturation Curves," *Petrophysics*, vol. 55(04), 2014, pp. 313-318.
34. J. J. Sheng, "Status of surfactant EOR technology," *Petroleum*, vol. 1(2), 2015, pp. 97-105.
35. C. Dai *et al.*, "Spontaneous Imbibition Investigation of Self-Dispersing Silica Nanofluids for Enhanced Oil Recovery in Low-Permeability Cores," *Energy & Fuels*, vol. 31(3), 2017, pp. 2663-2668.
36. S. Li and O. Torsaeter, "The Impact of Nanoparticles Adsorption and Transport on Wettability Alteration of Intermediate Wet Berea Sandstone," in *SPE Middle East Unconventional Resources Conference and Exhibition*, Muscat, Oman, 2015, pp. 14. https://doi.org/10.2118/172943-MS.
37. H. ShamsiJazeyi, C. A. Miller, M. S. Wong, J. M. Tour, and R. Verduzco, "Polymer-coated nanoparticles for enhanced oil recovery," *Journal of Applied Polymer Science*, vol. 131(15), 2014.
38. D. A. DiCarlo, B. Aminzadeh, M. Roberts, D. H. Chung, S. L. Bryant, and C. Huh, "Mobility control through spontaneous formation of nanoparticle stabilized emulsions," *Geophysical Research Letters*, vol. 38(24), 2011.